FULL PAPER

Dalton
www.rsc.org/dalton

Investigation of the mercury(II) coordination chemistry of tris[(1-methylimidazol-2-yl)methyl]amine by X-ray crystallography and NMR †

Deborah C. Bebout,*[a] Melissa M. Garland,[a] Geoffrey S. Murphy,[a] Edith V. Bowers,[a] Christopher J. Abelt[a] and Raymond J. Butcher[b]

[a] *Chemistry Department, The College of William & Mary, Williamsburg, VA 23187, USA. E-mail: dcbebo@wm.edu; Fax: 757 221 2715; Tel: 757 221 2558*

[b] *Chemistry Department, Howard University, Washington, DC 20059, USA. E-mail: rbutcher@howard.edu; Fax: 202 806 5442; Tel: 202 806 6886*

Received 3rd January 2003, Accepted 15th April 2003
First published as an Advance Article on the web 12th May 2003

The coordination chemistry of Hg(II) with tris[(1-methylimidazol-2-yl)methyl]amine (TMIMA) was investigated. The structures of $[Hg(TMIMA)_2](ClO_4)_2$ (**1**), $[Hg(TMIMA)(NCCH_3)](ClO_4)_2$ (**2**) and $[Hg(TMIMA)Cl]_2(HgCl_4)$ (**3**) were characterized by X-ray crystallography. Complex **1** has six strong $Hg–N_{imidazoyl}$ bonds ranging from 2.257(5) to 2.631(6) Å. Ligand geometry suggests the $Hg–N_{(NR_3)}$ distances of 2.959(6) Å in **1** reflects weak bonding interactions. This complex has a ^{199}Hg chemical shift of −1496 ppm, significantly upfield from nitrogen coordination complexes with lower coordination numbers. The five-coordinate complex **2** has $Hg–N_{(NR_3)}$, $Hg–N_{imidazoyl}$ and $Hg–N_{acetonitrile}$ bond lengths of 2.642(8), 2.198(5) and 2.264(11) Å, respectively. Complex **3** is also five coordinate, with $Hg–N_{(NR_3)}$, Hg–Cl and average $Hg–N_{imidazoyl}$ distances in the cations of 2.758(7), 2.424(2) and 2.29(4) Å, respectively. Conditions for slow exchange on the *J*(HgH) coupling time-scale were found for both 1 : 1 metal-to-ligand complexes in acetonitrile-d_3. Observed heteronuclear coupling constants were similar to those associated with Hg(II) substituted proteins with histidine–metal bonds. Solution and solid-state comparisons to the Hg(II) coordination chemistry of tetradenate pyridyl ligands are made. Relevance to development of ^{199}Hg NMR as a metallobioprobe is discussed.

Introduction

A wide variety of multidentate ligand systems have been used to simulate protein metal coordination environments. Many aromatic amines have been used in these ligands to emulate metal coordination by the 4-methylimidazoyl side chain of histidine, including various derivatives of pyridine, imidazole and pyrazole. Typically the coordination chemistry of the physiologically essential metal ions with each ligand is methodically investigated for both biomimetic behavior and similarity to the spectroscopic signatures of metals in protein coordination environments. These studies have provided considerable insight into the structure and function of numerous metalloproteins.

Recently we have been investigating the coordination chemistry of Hg(II) in biologically relevant ligand systems to investigate the potential of ^{199}Hg NMR as a metallobioprobe of proteins. The ideal metallobioprobe would have similar coordination properties to the native metal ion yet offer a sensitive alternative means of protein characterization. NMR is one of the most powerful spectroscopic techniques because it can provide specific bonding information. Since none of the physiologically essential metal ions has an isotope with favorable NMR properties, detailed NMR information about protein metal binding sites requires metal substitution. For example, a wide variety of Zn(II) proteins have been substituted with Cd(II) and investigated by ^{113}Cd NMR spectroscopy to gain valuable insight.[1] The wealth of information potentially available from NMR, including the identity of specific metal ligating amino acids, has motivated Cd(II) substitution of less similar metal ions as well. These studies have taken advantage of the limited coordination geometry preferences of d^{10} metal ions. Although also a d^{10} metal ion with a favorable isotope for NMR studies, Hg(II) has not been used extensively as a metallobioprobe. Development of ^{199}Hg NMR would complement ^{113}Cd NMR methods since the metals have different donor atom preferences. Furthermore, ^{199}Hg NMR has important advantages over ^{113}Cd NMR including shorter relaxation times,[2] larger and longer range heteronuclear coupling constants[3] and greater chemical shift dispersion. Hg(II) is slightly larger than Cd(II) and significantly larger than the physiologically essential metal ions. However, Hg(II) has been substituted for native Fe(II),[4] Cu(II)[2,5–7] and Zn(II)[5,8] ions without significant changes in overall protein structure or identity of the metal ligands.

Although rapid exchange is commonly associated with Hg(II) coordination chemistry, we have found that tri- and tetradentate amine ligands exhibit slow exchange behavior on the chemical shift time-scale under appropriate conditions. Our previous studies have focused on tripodal and dipodal amines with 2-methyl- and 2,6-dimethylpyridyl substituents.[9–12] The Mn(III),[13] Fe(III),[14] and Cu(II)[15] coordination chemistry of tris[2-(1-methylimidazol-2-yl)methyl]amine (TMIMA) has been investigated recently. Since the 1,2-dimethylimidazoyl substituents of these ligands are more similar to histidine than the pyridyl derivatives associated with ligands previously examined, we decided to compare the coordination properties of these ligands. In this paper we report the structures of $[Hg(TMIMA)_2](ClO_4)_2$ (**1**), $[Hg(TMIMA)(NCCH_3)](ClO_4)_2$ (**2**) and $[Hg(TMIMA)Cl]_2(HgCl_4)$ (**3**), the first structurally characterized complexes of Hg(II) with polyimidazoyl ligands. In addition, the acetonitrile-d_3 solution-state NMR of TMIMA in the presence of $Hg(ClO_4)_2$ and $HgCl_2$ is reported. These results are compared with previous studies of multidentate pyridyl ligands.

Experimental

Methods and materials

Starting materials were of commercially available reagent quality. Elemental analyses were carried out by Atlantic Microlab, Inc., Norcross, Georgia.

† Electronic supplementary information (ESI) available: Cell packing diagrams for **1**–**3** and NMR figures showing trends in chemical shift as a function of [Hg(II)]/**1** for both $Hg(ClO_4)_2$ and $HgCl_2$. See http://www.rsc.org/suppdata/dt/b3/b300001j/

DOI: 10.1039/b300001j

Table 1 Selected crystallographic data for **1**–**3**

Complex	$[Hg(TMIMA)_2](ClO_4)_2$ (**1**)	$[Hg(TMIMA)(NCCH_3)](ClO_4)_2$ (**2**)	$[Hg(TMIMA)Cl]_2(HgCl_4)$ (**3**)
Empirical formula	$C_{30}H_{42}Cl_2HgN_{14}O_8$	$C_{17}H_{24}Cl_2HgN_8O_8$	$C_{30}H_{42}Cl_6Hg_3N_{14}$
Formula weight	998.27	739.93	1413.25
Crystal system, space group	Monoclinic, $P2_1/c$	Rhombohedral, $R\bar{3}c$	Orthorhombic, *Pbna*
a/Å	12.3821(13)	12.3849(8)	9.093(3)
b/Å	13.6576(15)	12.3849(8)	15.381(4)
c/Å	12.5346(19)	57.739(4)	30.119(9)
α/°	90	90	90
β/°	110.358(9)	90	90
γ/°	90	120	90
V/Å^3	1987.3(4)	7669.4(9)	4213(2)
Z	2	12	4
D_c/Mg m^{-3}	1.668	1.922	2.228
Absorption coefficient/mm^{-1}	4.072	6.287	11.329
Temperature/K	296(2)	293(2)	168(2)
Independent reflections (R_{int})	4453 (0.0351)	1972 (0.0352)	4771 (0.0487)
$R1$,[a] $wR2$[b] [$I > 2\sigma(I)$]	0.0425, 0.0967	0.0391, 0.0924	0.0319, 0.0648
$R1$,[a] $wR2$[b] (all data)	0.0784, 0.1147	0.0824, 0.1108	0.0635, 0.0923

[a] $R1 = \Sigma||F_o| - |F_c||/\Sigma|F_o|$. [b] $wR2 = [\Sigma[w(F_o^2 - F_c^2)^2]/\Sigma[w(F_o^2)^2]]^{1/2}$.

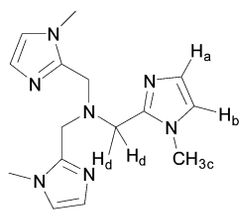

TMIMA

All of the perchlorate salts of mercury(II) complexes included in this work were stable for routine synthesis and purification procedures. However, caution should be exercised because perchlorate salts of metal complexes with organic ligands are potentially explosive.[16]

Synthesis of 1-methyl-2-imidazolecarbaldehyde oxime (MICAO)

MICAO was prepared by variation of the procedure of Oberhausen *et al.*[17] Hydroxylamine hydrochloride (19.0 g, 0.273 mol) and sodium carbonate (14.5 g, 0.137 mol) were dissolved in cold water. The solution was placed in an ice-bath and 1-methyl-2-imidazolecarbaldehyde (28.0 g, 0.255 mole) dissolved in ethanol (100 mL) was added dropwise. The solution was refluxed for 3 h then stored at 4 °C to precipitate the product. The white solid (29.5 g, 87%) isolated by vacuum filtration, rinsing with cold ethanol (30 mL) and drying in a vacuum desiccator was adequately pure for further manipulations; mp 168–170 °C (lit.,[17] 176 °C). δ_H (400 MHz; solvent DMSO-d_6; standard $SiMe_4$) 8.07 (1 H, s, CH_{oxime}), 7.27 (1 H, s, $CH_{imidazoyl}$), 7.00 (1 H, s, $CH_{imidazoyl}$), 3.82 (3 H, s, CH_3).

Synthesis of tris[2-(1-methylimidazol-2-yl)methyl]amine (TMIMA)

TMIMA was prepared from three equivalents of 1-methyl-2-imidazolecarbaldehyde by first converting two equivalents to the oxime MICOA[17] and preparing bis[2-(1-methylimidazol-2-yl)methyl]amine (BMIMA) by catalytic hydrogention.[18] BMIMA (1.0 g, 4.88 mmol) was added to a magnetically stirred solution of glacial acetic acid (1.25 mL, 21.8 mmol) and methanol (80 mL). A solution of 1-methyl-2-imidazolecarbaldehyde (0.73 g, 6.62 mmol) in methanol (40 mL) was added dropwise. The reaction mixture was cooled to 0 °C and sodium cyanoborohydride (1.38 g, 21.8 mmol) was added. After stirring for 18 h at 0 °C, the solution was acidified by addition of concentrated HCl. The reaction mixture was filtered to remove the white precipitate. The filtrate was concentrated *in vacuo* and dissolved in 30 mL water. Following extraction with diethyl ether (4 × 30 mL), the pH of the aqueous phase was adjusted above 9.0 with sodium carbonate and extracted with chloroform (4 × 30 mL). The combined organics were dried with $MgSO_4$, filtered, and concentrated *in vacuo* to a yellow solid. The solid was suspended in acetonitrile (2 mL), vacuum filtered, then dried to afford 339 mg (18%) of a white solid; mp 202.5–203.5 °C (literature value unavailable). δ_H (400 MHz; solvent CD_3CN; standard $SiMe_4$) 6.89 (3 H, d, J(HH) 1.3 Hz, H_b), 6.81 (3 H, d, J(HH) 1.4 Hz, H_a), 3.66 (6 H, s, H_d), 3.05 (9 H, s, H_c).

NMR measurements

Solutions for NMR analysis were prepared by adding stock solutions of mercuric salts in acetonitrile-d_3 to solutions of TMIMA or isolated complexes in acetonitrile-d_3 using calibrated autopipets. NMR spectra were recorded in 5-mm o.d. NMR tubes on a Varian Mercury 400VX operating in the pulse Fourier transform mode. The sample temperature was maintained by blowing chilled nitrogen over the NMR tube in the probe. Proton chemical shifts were measured relative to internal solvent but are reported relative to tetramethylsilane. Chemical shifts of ^{199}Hg were measured relative to an external reference of 0.1 M phenylmercuric acetate in acetonitrile-d_3 (−1439.5 ppm)[19] but are reported relative to dimethylmercury (0 ppm).

X-Ray crystallography

Selected crystallographic data are given in Table 1 and complete data are given in the CIF file. Data for **1** and **2** were collected at room temperature on a Siemens P4 four-circle diffractometer using a graphite-monochromated Mo-Kα X-radiation (λ = 0.71073 Å). During data collection three standard reflections were measured after every 97 reflections. Both crystals turned light gray in the beam, but the decay in the intensity of the standards was less than random error so no decay correction was performed on the data. Intensity data for **3** were collected on a Bruker SMART CCD diffractometer with graphite-monochromated Mo-Kα radiation (λ = 0.71073 Å) at −105 °C with absorption corrections performed using the SADABS program.[20] Although **3** turned light gray in the beam, re-collection of the initial 50 frames and analysis of these frames showed that no decay correction was needed. The structures were solved by direct methods[21] and refined on F^2 by full-matrix least-squares using the SHELXTL97 program package.[22] All non-hydrogen atoms were refined as anisotropic and, except as noted for the CH_3CN hydrogens of **2**, the hydrogen atomic positions were constrained in an idealized geometry relative to the bonded carbons and the isotropic thermal parameters were fixed.

Table 2 Selected bond distances (Å) and angles (°) in **1**–**3**

$[Hg(TMIMA)_2](ClO_4)_2$ (**1**)[a]		$[Hg(TMIMA)(NCCH_3)](ClO_4)_2$ (**2**)[b]		$[Hg(TMIMA)Cl]_2(HgCl_4)$ (**3**)[c]	
Hg–N	2.957(6)	Hg–N	2.642(8)	Hg–N	2.758(7)
Hg–N(1A)	2.631(6)	Hg–N(1)	2.198(5)	Hg–N(1A)	2.273(7)
Hg–N(1B)	2.257(5)	Hg–N(11)	2.264(11)	Hg–N(1B)	2.250(6)
Hg–N(1C)	2.537(5)			Hg–N(1C)	2.340(6)
				Hg–Cl	2.424(2)
N–Hg–N(1A)	59.8(2)	N–Hg–N(1)	71.83(11)	N–Hg–N(1A)	68.2(2)
N–Hg–N(1B)	63.5(2)	N–Hg–N(11)	180.00(2)	N–Hg–N(1B)	68.3(2)
N–Hg–N(1C)	60.5(2)	N(1)–Hg–N(1)	110.75(11)	N–Hg–N(1C)	67.9(2)
N–Hg–N(1AA)	120.2(2)	N(1)–Hg–N(11)	108.16(11)	N(1A)–Hg–N(1B)	119.4(2)
N–Hg–N(1BA)	116.5(2)	Hg–N(11)–C(11)	180.00(2)	N(1A)–Hg–N(1C)	101.5(2)
N–Hg–N(1CA)	119.5(2)			N(1B)–Hg–N(1C)	98.8(2)
N(1A)–Hg–N(1B)	100.37(19)			Cl–Hg–N	170.5(2)
N(1A)–Hg–N(1C)	99.59(17)			Cl–Hg–N(1A)	102.46(17)
N(1B)–Hg–N(1C)	96.31(18)			Cl–Hg–N(1B)	117.25(17)
N(1A)–Hg–N(1AA)[1]	180.0(2)			Cl–Hg–N(1C)	117.04(17)
N(1B)–Hg–N(1BA)[1]	180.0(4)				
N(1C)–Hg–N(1CA)[1]	180.0(3)				
N(1A)–Hg–N(1B)[1]	79.63(19)				
N(1A)–Hg–N(1C)[1]	80.41(17)				
N(1B)–Hg–N(1C)[1]	83.69(18)				

[a] Symmetry transformation used to generate equivalent atoms: $-x, -y+1, -z+1$. [b] Symmetry transformations used to generate equivalent atoms: $-x+y+1, -x+1, z; -y+1, x-y, z; x-y+1/3, -y+2/3, -z+7/6; -x+4/3, -y+2/3, -z+2/3; x-y+1/3, x-1/3, -z+2/3; y+1/3, -x+y+2/3, -z+2/3$. [c] Symmetry transformation used to generate equivalent atoms: $x, -y+1/2, -z+1$.

CCDC reference numbers 200560–200562.

See http://www.rsc.org/suppdata/dt/b3/b300001j/ for crystallographic data in CIF or other electronic format.

Preparation and X-ray diffraction of $[Hg(TMIMA)_2](ClO_4)_2$ (1). $Hg(ClO_4)_2 \cdot 3H_2O$ (75.7 mg, 0.167 mmol) was dissolved in 8 mL acetonitrile and TMIMA (100 mg, 0.334 mmol) was added. The solution was stirred and slowly diluted with 12 mL toluene and set aside for slow evaporation. Colorless X-ray quality crystals formed upon standing for five days. Crystals were collected by drawing off the mother liquor and air drying. Yield: 120 mg (28%); mp 229-230 °C (decomp.) (Found: C 36.06; H 4.18; N 19.48. $C_{30}H_{42}Cl_2HgN_{14}O_8$ requires C 36.09; H 4.24; N 19.63%); δ_H (400 MHz; solvent CD_3CN; standard $SiMe_4$; 2 mM; 20 °C) 6.98 (6 H, s, H_b), 6.50 (6 H, s, H_a), 4.02 (12 H, s, H_d), 3.60 (18 H, s, H_c); δ_{Hg} (71.588 MHz; solvent CD_3CN; standard 0.5 M phenylmercuric acetate in DMSO-d_6;[19] 50 mM with excess TMIMA; 20 °C) −1496.

A crystal measuring 0.25 × 0.75 × 0.55 mm was glued on the end of a glass fiber. The data were collected using the θ–2θ technique over a θ range of 2.98–27.5°. The final data to parameter ratio was 15 : 1.

Preparation and X-ray diffraction of $[Hg(TMIMA)(NCCH_3)](ClO_4)_2$ (2). $Hg(ClO_4)_2 \cdot 3H_2O$ (152 mg, 0.335 mmol) was dissolved in 8 mL acetonitrile and TMIMA (100 mg, 0.334 mmol) was added. Toluene (2.5 mL) was added slowly with stirring. The solution was set aside for slow evaporation. Colorless X-ray quality crystals formed upon standing for 4 days. Crystals were collected by drawing off the mother-liquor and air drying. Yield: 79 mg (32%); mp 205–207 °C (decomp.) (Found: C, 27.64; H, 3.18; N, 15.37. $C_{17}H_{24}Cl_2HgN_8O_8$ requires C, 27.59; H, 3.27; N, 15.14%); δ_H (400 MHz; solvent CD_3CN; standard $SiMe_4$; 2 mM; 20 °C) 7.18 (3 H, d, J(HH) 1.4 Hz, H_b), 7.08 (3 H, d, J(HH) = 1.4 Hz, H_a), 4.11 (6 H, s, H_d), 3.55 (9 H, s, H_c); (−40 °C) 7.18 (3 H, d, J(HH) 1.4 Hz, J(HgH) = 20 Hz, H_b), 7.05 (3 H, d, J(HH) = 1.4 Hz, J(HgH) 17 Hz, H_a), 4.03 (6 H, s, J(HgH) 7 Hz, H_d), 3.55 (9 H, s, H_c).

A crystal measuring 0.40 × 0.63 × 0.59 mm was glued on the end of a glass fiber. The data were collected using the θ–2θ technique over a θ range of 2.03–27.50°. The final data to parameter ratio was 14 : 1.

Preparation and X-ray diffraction of $[Hg(TMIMA)Cl]_2(HgCl_4)$ (3). $HgCl_2$ (158 mg, 0.334 mmol) was dissolved in 8 mL acetonitrile and TMIMA (100 mg, 0.334 mmol) was added. Toluene (2.5 mL) was added slowly with stirring. The solution was separated into 2 mL aliquots and set aside for slow evaporation. Upon standing for one week, some vials contained colorless plates (mp 210–212 °C (decomp.)) and others contained colorless needles suitable for X-ray crystallography (mp 215–217 °C (decomp.)). Crystals were collected by drawing off the mother-liquor and air drying. Yield 88 mg (28%). The two crystal types were indistinguishable by NMR (Found C, 26.18; H, 3.13; N, 13.90. $C_{30}H_{42}Cl_6Hg_3N_{14}$ requires C, 25.50; H, 2.99; N, 13.88%); δ_H (400 MHz; solvent CD_3CN; standard $SiMe_4$; 2 mM; 20 °C) 7.13 (6 H, d, J(HH) 1.5 Hz, H_b), 6.99 (6 H, d, J(HH) 1.5 Hz, H_a), 4.02 (12 H, s, H_d), 3.58 (18 H, s, H_c); (−40 °C) 7.15 (6 H, d, J(HH) 1 Hz, J(HgH) 10 Hz, H_b), 6.95 (6 H, d, J(HH) 1 Hz, J(HgH) = 9 Hz, H_a), 4.01 (12 H, s, J(HgH) = 11 Hz, H_d), 3.55 (18 H, s, H_c).

A crystal measuring 0.08 × 0.12 × 0.30 mm was glued on the end of a glass fiber. The data were collected using the θ–2θ technique over a θ range of 1.35–28.33°. The final data to parameter ratio was 20 : 1.

Results

The structures of $[Hg(TMIMA)_2](ClO_4)_2$ (**1**), $[Hg(TMIMA)(NCCH_3)](ClO_4)_2$ (**2**) and $[Hg(TMIMA)Cl]_2HgCl_4$ (**3**) are reported herein. Selected bond distances and bond angles are given in Table 2.

Crystal structure and solution-state NMR of $[Hg(TMIMA)_2](ClO_4)_2$ (1). The Hg(II) ion is located at an inversion center within a bicapped trigonal antiprism of nitrogen atoms (D_{3d} core symmetry, D_3 ion symmetry) (Fig. 1). The overall conformation of the ligand indicates that the lone pairs of all eight nitrogens are directed towards the metal center. The $Hg–N_{(NR_3)}$ distances of 2.957(6) Å are fairly long, but shorter than the sum of the van der Waals radii (r_{vdw}(N) = 1.60 Å,[23] r_{vdw} (Hg) = 1.73–2.00 Å).[24] The $Hg–N_{imidazoyl}$ bonds form a trigonal antiprism and are significantly shorter, consistent with differences in donor capacity, the steric demands of ligand architecture, cooperative optimization of ligand–metal interactions and adjustments for interactions between opposing ligands. The

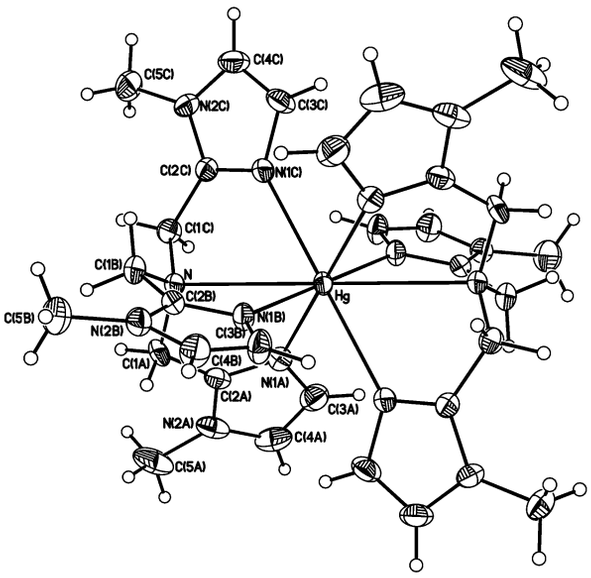

Fig. 1 Thermal ellipsoid plot of the $[Hg(TMIMA)_2]^{2+}$ cation of **1**. Ellipsoids are at 50% probability. Only one ligand has been completely labeled.

$Hg–N_{imidazoyl}$ bond distances range from 2.259(6) to 2.628(7) Å, bracketing the Hg–N distance for the one structurally characterized complex of Hg(II) with a simple imidazole derivative (2.45 Å)[25] and the range of Hg–N distances to histidine imidazoyl groups in Hg(II) substituted proteins (2.3–2.5 Å).[7] Since the previously reported complexes of Hg(II) with imidazoyl derivatives are all four coordinate, longer $Hg–N_{imidazoyl}$ bonds are expected in **1**. A reason for the short $Hg–N_{imidazoyl}$ bond length in **1** was not readily apparent.

This is the first 1 : 2 metal-to-ligand complex of TMIMA to be structurally characterized. In addition, there are very few structurally characterized high coordination number complexes of Hg(II) in which all the donor nitrogens are part of chelating organic ligands. Previous investigation of Hg(II) coordination chemistry with a potentially tetradentate tripodal nitrogen ligand provided the complex $[Hg(TMPA)_2](ClO_4)_2$ (**4**, TMPA = tris[(2-pyridyl)methyl]amine).[12] While the symmetries and formal coordination numbers of **4** and **1** are similar, the $Hg–N_{(NR_3)}$ distance in **4** is 2.560(3) Å, slightly shorter than the average $Hg–N_{pyridyl}$ distance of 2.583(8) Å. Hence, in Grdenic terminology,[26] **1** is the first example of characteristic 6 coordination and effective 8 coordination for a nitrogen coordination compound of Hg(II).

The solution-state behavior of a dilute CD_3CN solution of complex **1** was also investigated for comparison with **4**. In solution, **1** exhibits a single set of resonances for the four proton types indicating effective three-fold symmetry through rapid solution exchange processes which eliminate the differences between the $Hg–N_{imidazoyl}$ groups observed in the solid state. Proton chemical shift properties were comparable for **1** and **4**,[12] including fluxionally exchanged methylene protons, shielding of the protons closest to the binding aromatic nitrogens by the ring current of the opposing ligand, and deshielding of remaining ligand resonances by σ donation to the metal cation. However, ligand proton chemical shifts were inversely dependent on the metal-to-ligand ratio below $[Hg(ClO_4)_2]$/[TMIMA] = 0.5 and then increased at higher metal-to-ligand ratio, reflecting the precedented solution speciation of tripodal tetradentate amines with $Hg(ClO_4)_2$ (ESI, †Fig. S2).[9,12] Rapid intermolecular exchange processes with free ligand and higher metal-to-ligand ratio complexes precluded detection of J(HgH) for **1**. In contrast, extensive heteronuclear coupling between ligand protons and Hg was detected for **4** in the presence of excess ligand.

Additional investigations of **1** were conducted by solution-state ^{199}Hg NMR. No resonances were detected for 20–50 mM solutions of **1** in CD_3CN, possibly due to the complexity of solution equilibria at [Hg(II)]/[TMIMA] = 0.5 (*vide supra*; Fig. S2). However, in the presence of excess ligand a ^{199}Hg resonance was detected at −1496 ppm. Previous studies have suggested that ligand exchange for complexes of type HgL_2 involves an associative exchange mechanism.[9,12] The ligand proton chemical shifts were linearly dependent on the metal-to-ligand ratio for [Hg(II)]/[TMIMA] < 0.375 (Fig. S2). This indicates that the lower metal-to-ligand ratio complex(es) involved in ligand exchange with $[Hg(TMIMA)_2]^{2+}$ are kinetically accessible but thermodynamically unstable. The position of the ^{199}Hg peak was independent of the amount of excess ligand present confirming the transient existence of lower metal-to-ligand ratio complexes and permitting assignment of the ^{199}Hg peak observed to $[Hg(TMIMA)_2]^{2+}$.

Crystal structure and solution-state NMR of $[Hg(TMIMA)(NCCH_3)](ClO_4)_2$ (2). The coordination sphere of Hg(II) has three-fold symmetry in **2** (Fig. 2). The TMIMA ligand is tetradendate and the acetonitrile is *trans* to the amine nitrogen, thus forming a distorted trigonal bipyramid (C_{3v} core symmetry, C_3 ion symmetry). As expected for a lower coordination number complex, the $Hg–N_{imidazoyl}$ and Hg–N distances are shorter than those found in **1**. However, in **2** the $Hg–N_{(NR_3)}$ bond lengths are still significantly longer than the $Hg–N_{imidazoyl}$ bond lengths (0.444 Å) consistent with the reduced donor capacity of aliphatic nitrogens in comparison with imidazoyl nitrogens as well as the steric demands of ligand architecture. Cooperative optimization of ligand–metal interactions with the large Hg^{2+} ion also likely contributes to the elongation of the metal-$N_{(NR_3)}$ bonds in **2**.

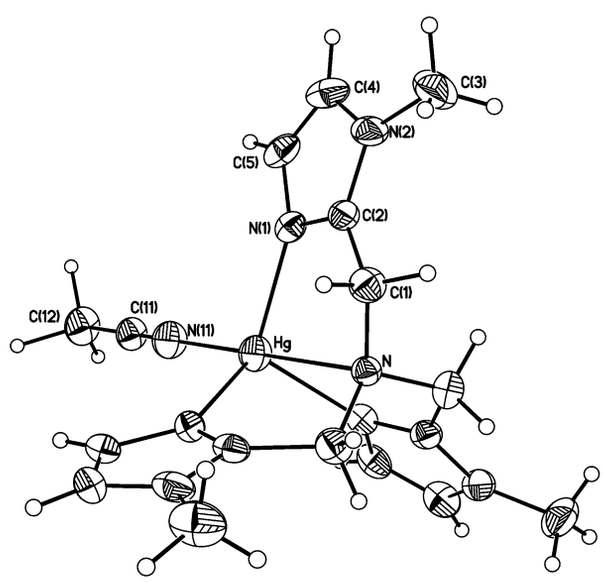

Fig. 2 Thermal ellipsoid plot of the $[Hg(TMIMA)(NCCH_3)]^{2+}$ cation of (**2**). Ellipsoids are at 50% probability. Only one (1-methylimidazol-2-yl)methyl group has been completely labeled.

This structure can be compared to the one other reported five-coordinate complex of TMIMA and other five-coordinate complexes of Hg(II) involving potentially tetradentate amines, as well as Hg(II) substituted proteins. The $Cu–N_{(NR_3)}$ and average $Cu–N_{imidazoyl}$ bond lengths in $[Cu(TMIMA)Cl]PF_6 \cdot CH_3CN$[15] are 2.167 and 2.03 Å, respectively, a difference of approximately 0.14 Å. In this copper complex, the axial Cl is 2.234 Å from the metal ion,[15] comparable to the $Hg–N_{acetonitrile}$ bond distance in **2**. The differences between $Hg–N_{(NR_3)}$ and $Hg–N_{pyridyl}$ distances of five-coordinate complexes involving tripodal amines with pyridyl donors have been small as well. In $[Hg(TMPA)Cl]_2(HgCl_4)$[12] and $[Hg(TLA)Cl]_2(Hg_2Cl_6)$[10] (TLA = tris[(2-(6-methylpyridyl))methyl]amine), the average $Hg–N_{(NR_3)}$

bond length was smaller than the average Hg–$N_{pyridyl}$ bond length by only 0.040 and 0.132 Å, respectively. The average Hg–Cl distance is 2.355 Å and 2.366 Å, respectively, in these cations, slightly longer than the Hg–$N_{acetonitrile}$ bond distance in **2**. The 2.198(8) Å Hg–$N_{imidazoyl}$ bond length in **2** is below the range of Hg–N distances to histidine imidazoyl groups in four-coordinate Hg(II) substituted proteins (2.3–2.5 Å).[7]

Complex **2** exhibited a single set of proton resonances for each type of ligand proton in 2 mM CD_3CN solutions indicating preservation of three-fold symmetry and fluxionally equivalent methylene protons. Ligand protons were deshielded 0.24–0.50 ppm through σ donation to Hg(II). At room temperature, dilute solutions of complex **2** exhibited the fast exchange behavior on the coupling constant time-scale usually associated with Hg(II) complexes due to the equilibrium formation of complexes with lower metal-to-ligand ratios (ESI, †Fig. S2). However, slow exchange conditions on the coupling constant time-scale could be achieved by cooling the sample to −40 °C (Fig. 3) or by addition of a 5% excess of $Hg(ClO_4)_2$ at 20 °C. Coupling of ^{199}Hg to both of the imidazoyl protons and the methylene protons was apparent. Coupling satellites had the same multiplicity as the parent resonance and appeared to be approximately one-fifth the size of the main resonance consistent with the 16.8% natural abundance of ^{199}Hg. Interestingly, the coupling expected to be generated predominantly through a three-bond pathway to H_a was 17 Hz while the coupling to H_b, for which only four- and five-bond coupling pathways are available, was 20 Hz. Since *J*(HgH) are precedented over four and five bonds for nitrogen coordination compounds of Hg(II),[9] the larger longer range coupling may reflect additive contributions from both potential pathways. The methylene protons of **2** were also coupled to Hg with *J*(HgH) 7 Hz. These heteronuclear coupling constants are somewhat smaller that those recently reported for Hg(II) complexes of other potentially tetradentate amines,[9,10,12] but comparable in magnitude to those reported for Hg(II) substituted proteins.[4–6]

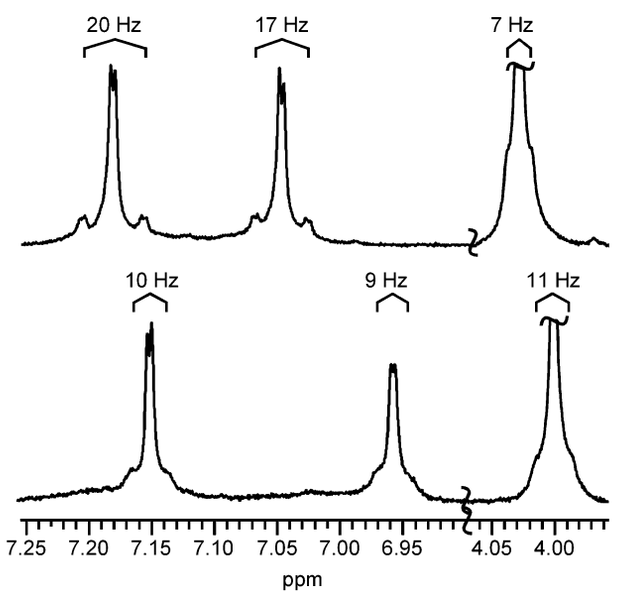

Fig. 3 Proton NMR spectra recorded in CD_3CN for nominally 2 mM **2** at −40 °C (upper) and nominally 0.8 mM **3** at −40 °C with 15% excess $HgCl_2$ added (lower). Singlet resonances without ^{199}Hg coupling satellites for the methyl protons at 3.55 ppm for both complexes are not shown. Magnitudes of *J*(HgH) are indicated.

Characterization of **2** by ^{199}Hg NMR was attempted with 20–68 mM CD_3CN solutions. These samples did not exhibit slow exchange on the *J*(HgH) time-scale at −40 °C. Furthermore, addition of excess $Hg(ClO_4)_2$ to these solutions resulted in formation of a white precipitate and appearance of additional peaks in the proton NMR spectrum precluding meaningful characterization.

Crystal structure and solution-state NMR of [Hg(TMIMA)-$Cl]_2HgCl_4$ (3). There are two identical five-coordinate [Hg(TMIMA)Cl]$^+$ ions and a nearly tetrahedral $[HgCl_4]^{2-}$ anion in the asymmetric unit of **3** (Fig. 4). Although the Hg–$N_{(NR_3)}$ distance of 2.758(7) Å is fairly long, it is significantly shorter than the sum of the van der Waals radii[23,24] and the overall conformation of the ligand indicates that the lone pair on the aliphatic nitrogen is directed towards the metal center for a bonding interaction. The Hg(II) coordination environment is distorted trigonal bipyramidal with the chloride *trans* to the aliphatic nitrogen. The Hg–Cl distance of 2.424(2) Å in the cation is slightly longer than the average Hg–Cl distances found in the cations of related complexes $[Hg(TMPA)Cl]_2(Hg_2Cl_6)$ (2.354(12) Å)[12] and $[Hg(TLA)Cl]_2(Hg_2Cl_6)$ [2.366(8) Å].[10] Although the overall geometry of **3** is very similar to **2**, the metal–ligand bond lengths are uniformly larger. The Hg–$N_{imidzoyl}$ bond lengths are similar (average 2.29(4) Å), bracketing the lower end of the range of Hg–N distances to histidine imidazoyl groups in Hg(II) substituted proteins (2.3–2.5 Å).[7]

In CD_3CN solution, **3** gave rise to a single set of (1-methylimidazol-2-yl)methyl proton resonances consistent with expected three-fold symmetry and exchange averaged methylene protons. The resonances were shifted downfield 0.17–0.53 ppm with respect to free ligand with generally the same trend as observed for **2**. The ligand chemical shifts were linearly dependent on the metal-to-ligand ratio below $[HgCl_2]$/[TMIMA] = 1.0 (ESI, †Fig. S3), indicating that a 1 : 1 metal-to-ligand complex was the most thermodynamically stable TMIMA complex of $HgCl_2$. Although the metal-to-ligand ratio in **3** is 1.5 and the neutral complex $[Hg(TMIMA)Cl_2]$ is potentially consistent with the NMR data, isolation of **3** from a 1 : 1 metal-to-ligand ratio solution indicates [Hg(TMIMA)Cl]$^+$ is present under these conditions. The later is consistent with the NMR assuming both that ion pairing is negligible and that the cation is formed by a dissociative process which is independent of the presence of excess $HgCl_2$ as opposed to an equilibrium of type (1).

$$2[HgLCl_2] + HgCl_2 \rightleftharpoons 2[HgLCl]^+ + HgCl_4^{2-} \quad (1)$$

The above equilibrium was evident with the more sterically demanding ligand TLA. The neutral complex $[Hg(TLA)Cl_2]$, in which one of the lutidyl arms is pendant, was prevalent at [Hg]/[TLA] = 1 and [Hg(TLA)Cl]$^+$ was prevalent at [Hg]/[TLA] > 1.5.[10] Interestingly, with TMPA chemical shift discontinuities at $[HgCl_2]$/[TMPA] = 0.5 and 1.0 indicated that [Hg(TMPA)Cl]$^+$ was less thermodynamically stable than a 1 : 2 complex.[12]

At −40 °C, slow exchange conditions on the coupling constant time-scale were found for 2 mM **3** in CD_3CN (Fig. 3). As in **2**, comparable heteronuclear coupling constants were observed between ^{199}Hg and both imidazoyl protons. Heteronuclear couplings of 10 and 11 Hz were detected to H_a and H_b, respectively. Interestingly, **3** had a longer Hg–$N_{(NR_3)}$ bond than **2**, yet was associated with a stronger heteronuclear coupling constant to the methylene protons (*J*(HgH) 11 Hz). The limited solubility of **3** in CD_3CN thwarted attempts to investigate it by ^{199}Hg NMR.

Discussion

Tetradentate binding modes for TMIMA were found for three complexes of Hg(II) in the solid state. Although related tripodal amines with pyridyl donors were observed to have comparable Hg–N distances for all donors, the TMIMA complexes generally had significantly longer distances to the aliphatic nitrogen than the imidazoyl nitrogens. The same trend has been observed with the five previously reported complexes of TMIMA,

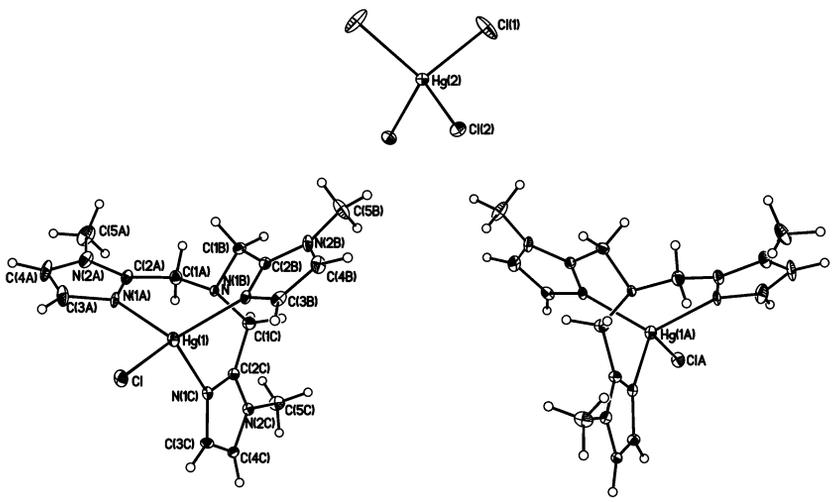

Fig. 4 Thermal ellipsoid plot of $[Hg(TMIMA)Cl]_2(HgCl_4)$ (**3**). Ellipsoids are at 50% probability. Only one $[Hg(TMIMA)Cl]^+$ has been completely labeled.

although the differences have been less substantial,[13–15] reflecting differences in ion size and hardness. The shorter Hg–$N_{imidazoyl}$ bonds are consistent with the stronger σ and π donor ability of imidazoyl nitrogen compared to pyridyl and aliphatic nitrogen. Furthermore, the metal chelate ring C–N double bond is slightly shorter with imidazoyl donors than pyridyl donors leading to additional architectural constraints on chelation. Stronger binding to the aromatic amines enhances the biorelevance of TMIMA in comparison to related pyridyl ligands since histidine is much more common in protein metal binding sites than lysine.

Although correlations between solid-state structures and solution-state NMR properties must always be made carefully,[27] the symmetry of tripodal ligands facilitates interpretation of spectra within the context of crystallographic structures. In CD_3CN solution, each complex gave rise to a single set of four proton resonances indicating three-fold symmetry on the chemical shift time-scale. Although **1** and **3** are not three-fold symmetric in the solid-state, packing effects that disrupt complex symmetry would be absent in solution.

The trends in proton chemical shift as a function of the metal-to-ligand ratio complemented structure assignments. The observed trends for the perchlorate system (ESI, †Fig. S2) were consistent with the series of linked equilibria established for related tetradentate amines,[9,12] in the context of the lower steric demands of TMIMA. For the chloride system, the proton NMR behavior was consistent with the prevalence of either $[Hg(TMIMA)Cl_2]$ or $[Hg(TMIMA)Cl]^+$ in solution, assuming ion pairing was negligible for the later.

Slow exchange conditions on the *J*(HgH) time-scale were found for the two lower coordination number complexes of TMIMA. In general, the heteronuclear coupling constants observed for TMIMA complexes were smaller than those observed with related pyridyl ligand systems and more comparable to those observed for Hg(II) substituted proteins. There are many contributing factors to the magnitudes of indirect nuclear spin–spin coupling constants including electronegativity of substituents, hybridization, bond angles and bond lengths. Coupling between ^{199}Hg and nuclei up to five bonds away has been observed in Hg(II) coordination compounds with nitrogen ligands[9] (seven bonds away in alkylmercurials[28]). Although there is no standard theory to explain long-range couplings, it is generally accepted that coupling constants are additive, which can lead to significant enhancements if contributions are of the same sign. Additivity over as many as five bonds is proposed to account for the comparable magnitudes of ^{199}Hg coupling constants to H_a and H_b. Neither **2** nor **3** proved to be suitable for characterization by ^{199}Hg NMR spectroscopy due to solubility related issues.

Although slow exchange conditions on the *J*(HgH) time-scale were inaccessible for **1** due to rapid ligand exchange, the complex was characterizable by solution-state ^{199}Hg NMR. Solid-state ^{199}Hg NMR is preferable for characterization of Hg(II) coordination compounds to avoid exchange complications.[5] However, the concentration independent −1496 ppm ^{199}Hg chemical shift of **1** in the presence of excess ligand supported the structural assignment. The ^{199}Hg chemical shift of **1** is approximately 450 and 250 ppm upfield of the ^{199}Hg chemical shifts for $[Hg(N(SiMe_3))_2]$ and $[Hg(ethylenediamine)_2]^{2+}$, respectively, the only nitrogen coordination compounds of Hg(II) for which ^{199}Hg chemical shifts have apparently been reported.[28,5] Interestingly, the ^{199}Hg chemical shift of **4** is −1996 ppm in CD_3CN at 20 °C.[29] Both **1** and **4** are formally eight coordinate but in **1** the axial Hg–N_{amine} bonds are significantly longer than the Hg–$N_{imidazoyl}$ bonds while in **4** all Hg–N are comparable. Increases in coordination number are associated with upfield shifts in ^{199}Hg resonance positions with other ligand types.[28]

Conclusions

Generally ligands with pyridyl donors have been exploited much more extensively than ligands with imidazoyl donors in bioinorganic model studies, in part due to differences in ease of synthesis and stability. However, there are clearly significant differences in electronics and sterics of these aromatic amines. The three structures reported in this work highlight the differences in donor capacity of imidazoyl and aliphatic amine ligands as well as the demanding sterics of five-membered chelate rings involving imidazoyl donors. Additional studies of TMIMA and related ligands with physiologically essential metal ions would complement the existing literature.

Heteronuclear coupling is not routinely observed between ^{199}Hg and protons of small organic ligands in solution, even with multidentate ligands. However, each of the tripodal ligand systems with pyridyl and imidazoyl donors we have investigated has permitted detection of *J*(HgH) for two or more specific complexes. The magnitudes of *J*(HgH) observed with TMIMA were more comparable to the magnitudes of *J*(HgH) observed in Hg(II) substituted proteins.[4–6] These results encourage investigation of the Hg(II) coordination chemistry of additional tripodal ligand systems involving imidazoyl donors, as well as ligand systems with more diverse donors. In addition, tripodal ligand systems may advance solution-state NMR studies of other high natural abundance spin $I = ½$ nuclei, such as

^{109}Ag, for which heteronuclear coupling with protons of organic ligands are rarely observed.

Acknowledgements

We thank Monte Helm for helpful discussions regarding ^{199}Hg NMR and Robert Hinkle for assisting with the NOE experiments to confirm proton assignments. This research was supported by a Bristol–Meyers Squibb Company award of Research Corporation and NIH AREA award number 1R15GM59043–01. E. V. B. was supported in part by a Howard Hughes Medical Institute grant through the Undergraduate Biological Sciences Education Program to the College of William and Mary and a Beckman Foundation Research Scholarship. M. M. G. was supported in part by a Batten Scholarship for Pre-Honors Research Summer Fellowship from the College of William and Mary. The NSF chemical instrumentation program partially funded purchase of the NMR instrumentation. R. J. B. acknowledges the DoD-ONR instrumentation program for funds to upgrade the Siemens P4 diffractometer and the NIH-MBRS program for funds to maintain this diffractometer. We are thankful to Dr Travis Holman for permitting us to use a Bruker SMART 1K CCD for diffraction analysis of **3**.

References

1 M. F. Summers, *Coord. Chem. Rev.*, 1988, **86**, 43–134; P. D. Ellis, *Science*, 1983, **221**, 1141–1146.
2 L. M. Utschig, J. G. Wright, G. Dieckmann, V. Pecoraro and T. V. O'Halloran, *Inorg. Chem.*, 1995, **34**, 2497–2498.
3 D. C. Bebout, S. W. Stokes and R. J. Butcher, *Inorg. Chem.*, 1999, **38**, 1126–1133.
4 P. R. Blake, B. Lee, M. F. Summers, J.-B. Park, Z. H. Zhou and M. W. W. Adams, *New J. Chem.*, 1994, **18**, 387–395.
5 L. M. Utschig, J. W. Bryson and T. V. O'Halloran, *Science*, 1995, **268**, 380–385.
6 L. M. Utschig, T. Baynard, C. Strong and T. V. O'Halloran, *Inorg. Chem.*, 1997, **36**, 2926–2927.
7 F. X. Gomis-Rueth, F. Grams, I. Yiallouros, H. Nar, U. Kuesthardt, R. Zwilling, W. Bode and W. Stoecker, *J. Biol. Chem.*, 1994, **269**, 17111–17117; W. B. Church, J. M. Guss, J. J. Potter and H. C. Freeman, *J. Biol. Chem.*, 1986, **261**, 234–237.
8 D. C. Rees, J. B. Howard, P. Chakrabarti, T. Yeats, B. T. Hsu, K. D. Hardman and W. N. Lipscomb, in *Zinc Enzymes*, ed. I. Bertini, C. Luchinat, W. Maret and M. Zeppezauer, Birkhäuser Verlag, Basel, 1986, p. 155.
9 D. C. Bebout, J. F. Bush II, K. K. Crahan, E. V. Bowers and R. J. Butcher, *Inorg. Chem.*, 2002, **41**, 2529–2536.
10 D. C. Bebout, J. F. Bush II, K. K. Crahan, M. E. Kastner and D. A. Parrish, *Inorg. Chem.*, 1998, **37**, 4641–4646.
11 D. C. Bebout, A. E. DeLanoy, D. E. Ehmann, M. E. Kastner, D. A. Parrish and R. J. Butcher, *Inorg. Chem.*, 1998, **37**, 2952–2959.
12 D. C. Bebout, D. E. Ehmann, J. C. Trinidad, K. K. Crahan, M. E. Kastner and D. A. Parrish, *Inorg. Chem.*, 1997, **36**, 4257–4264.
13 K. J. Oberhausen, R. J. O'Brein, J. F. Richardson, R. M. Buchanan, R. Costa, J.-M. Latour, H.-L. Tsai and D. N. Hendrickson, *Inorg. Chem.*, 1993, **32**, 4561–4565.
14 J. Wang, M. S. Mashuta, Z. Sun, J. F. Richardson, D. N. Hendrickson and R. M. Buchanan, *Inorg. Chem.*, 1996, **35**, 6642–6643; R. M. Buchanan, S. Chen, J. F. Richardson, M. Bressan, L. Forti, A. Morvillo and R. H. Fish, *Inorg. Chem.*, 1994, **33**, 3208–3209; R. H. Fish, M. S. Konings, K. J. Oberhausen, R. H. Fong, W. M. Yu, G. Christou, J. B. Vincent, D. K. Coggin and R. M. Buchanan, *Inorg. Chem.*, 1991, **30**, 3002–3006.
15 K. J. Oberhausen, R. J. O'Brien, J. F. Richardson and R. M. Buchanan, *Inorg. Chim. Acta*, 1990, **173**, 145–154.
16 W. C. Wosley, *J. Chem. Educ.*, 1973, **50**, A335; K. N. Raymond, *Chem. Eng. News*, 1983, **61**(49), 4.
17 K. J. Oberhausen, J. F. Richardson, R. M. Buchanan and W. Pierce, *Polyhedron*, 1989, **8**, 659–668.
18 M. Rodriguez, I. Morgenstern-Badarau, M. Cesario, J. Guilhem, B. Keita and L. Nadjo, *Inorg. Chem.*, 1996, **35**, 7804–7810.
19 M. Borzo and G. E. Maciel, *J. Magn. Reson.*, 1975, **19**, 279–282.
20 G. M. Sheldrick, SADABS, Program for Empirical Absorption Correction of Area Detector Data; University of Göttingen, 1996.
21 G. M. Sheldrick, SHELXS 97, Program for Crystal Structure Solution; University of Göttingen, 1997.
22 G. M. Sheldrick, SHELXL 97, Program for Crystal Structure Refinement; University of Göttingen, 1997.
23 S. C. Nyburg and C. H. Faerman, *Acta Crystallogr., Sect. B*, 1985, **41**, 274–279.
24 A. J. Canty and G. B. Deacon, *Inorg. Chim. Acta*, 1980, **45**, L225–L227.
25 F. H. Allen, J. E. Davies, J. J. Galloy, O. Johnson, O. Kennard, C. F. Macrae, E. M. Mitchell, G. F. Mitchell, J. M. Smith and D. G. Watson, *J. Chem. Inf. Comput. Sci.*, 1991, **31**, 187–204; Z. Popovic, D. Matkovic-Calogovic, Z. Soldin, G. Pavlovic, N. Davidovic and D. Vikic-Topic, *Inorg. Chim. Acta*, 1999, **294**, 35–46.
26 D. Grdenic, *Quart. Rev.*, 1965, **19**, 303–328.
27 J. A. Davies and S. Dutremez, *Coord. Chem. Rev.*, 1992, **114**, 201–247.
28 B. Wrackmeyer and R. Contreras, *Annu. Rep. NMR Spectrosc.*, 1992, **24**, 267–329.
29 D. C. Bebout, unpublished result.